Assessment Method Of Farmland Heavy Metal Content Based On Improved Elman And GWO Algorithm

Hui Zhang[1*], Lu Qiao[1], Weifeng Han[2], Benyin Li[2], and Yanfen Li[3]

[1] Henan Academy of Agricultural Sciences, Institute of Agricultural Economics and Rural Development, Zhengzhou 450002, China
[2] Henan Academy of Agricultural Sciences, Institute of Plant Nutrition and Resource Environment, Zhengzhou, Henan, China
[3] Academy of Agricultural and Forestry Sciences (Jiaozuo), Jiaozuo, Henan, China
[*] Corresponding author. E-mail: yanni1358877@126.com

Received: Mar. 04, 2026; Accepted: May. 25, 2026

Abstract: This study proposes a composite evaluation model based on improved Elman and mixed optimization strategy to address the core issues of insufficient dynamic sequence modeling ability, incomplete capture of multi factor nonlinear interaction relationships, and model parameters easily falling into local optima in existing methods for assessing heavy metal content in farmland soils. High precision dynamic evaluation of soil heavy metal content has been achieved by integrating gated loop units to improve random forest, convolutional block attention mechanism, and grey wolf optimizer and genetic algorithm to improve particle swarm optimization algorithm. The results showed that the evaluation accuracy of the CRF PGElman model reached 99.7%, with an error rate of 2.5%, an average absolute error of 0.21mg/kg, a root mean square error of 0.33mg/kg, and an R^2 of 0.97. In cross regional validation, the model achieved recognition accuracies of 0.99, 0.98, and 0.99 for iron, chromium, and mercury, respectively. The research contribution lies in the construction of an intelligent hybrid assessment framework, which provides a new technological path for monitoring heavy metal pollution in farmland soil and quantifiable accuracy improvement for assessing heavy metal content in farmland soil under different geographical regions and pollution backgrounds. It has deployment value in practical monitoring applications.

Keywords: Assessment; Elman; Farmland heavy metal content; GRU; GWO; PSO

http://dx.doi.org/10.6180/jase.202610_33.029

1. Introduction

Accurate appraisal of the content of heavy metals in farmland is crucial for the healthy development of agriculture, as it directly affects not only the quality of agricultural products but also the protection of soil ecological environment [1]. However, with the advance of appraisal technologies, the accuracy requirement of farmland heavy metal content appraisal is growing. The traditional appraisal technique mainly involves single physical and chemical tests as well as basic statistics. However, those traditional techniques have many defects, such as the possibility of large appraisal errors, which prevents real-time appraisal during application [2]. Therefore, efficient and accurate appraisal of farmland heavy metal content has been a focus of agricultural environmental protection and soil science studies. The fast development of intelligent technologies provides a new prospect for models of deep learning, which offers a new solution for the problem of farmland heavy metal content appraisal [3]. The Elman Neural Network (Elman) is a type of recurrent neural network that stores the historical output information of the hidden layer by setting a context layer, enabling it to process dynamic sequence data [4]. The Grey Wolf Optimizer (GWO) is an intelligent optimization algorithm simulating wolf hunting behaviors, finding optimal solutions by modeling the search and attack behaviors of a wolf pack [5]. Therefore, the study combines GWO with Elman neural networks to form the GElman algorithm. Among them, GWO simulates the search and attack mechanisms in wolf pack predation behavior to globally optimize the key parameters of the Elman model, thereby avoiding the problem of traditional parameter initialization methods easily falling into local optima. This optimization mechanism can enhance the fitting ability of Elman network to the dynamic changes and nonlinear characteristics of soil heavy metal content, enabling the model to more accurately capture the complex mapping relationship between heavy metal elements and environmental factors in the evaluation process. Compared with traditional algorithms for processing sequences, Elman yielded prominent advantages, having higher dynamic memory power for sequences and simulating correlations in sequences more accurately. Elman proved its considerable value in various testing domains, thus gaining significant attention from scholars at home and abroad. To properly predict the degree of water turbidity, Wang, et al., presented a model based upon the combination of Random Forest and Elman. They obtained multi-dimensional data for water quality, made feature selections by using Random Forest, trained a model based upon these feature variables in Elman, and finally achieved the predicted outcomes [6]. For lithium battery health assessment, Xiong et al. proposed a model combining Cuckoo Search and Elman. They used the global optimization capability of Cuckoo Search to determine the network parameters of Elman, enhancing its ability to analyze battery state data and accurately evaluate battery health [7]. Balamurugan et al. proposed an encryption-enhanced Elman method to improve cloud computing security. The method embedded encryption into Elman to process dynamic verification data integrity, ensuring data security throughout the process [8]. GWO improved the assessment accuracy and the depth of data correlation through its global optimization capability and efficient convergence when optimizing network parameters. For the prediction of concrete compressive strength, a model based on Support Vector Machine (SVM) and GWO was adopted by Ahmed et al. GWO was used for the optimization of the SVM parameters, and the developed prediction model was trained with input examples and the concrete compressive strength was predicted from the optimized model [9]. For the fulfillment of more accurate grade points on the production line, a model based on the integration of GWO was developed by Yongjie et al. The grade points were identified based on the features obtained from the integrated algorithms, and the grade points were accurately identified [10]. The evaluation of heavy metals in farmland soil is often utilized as an index to measure soil ecological safety. The accurate evaluation index provides an effective reference to prevent contamination, while large deviations between evaluation standards may affect remediation. This issue has been researched from different perspectives by various scientists. To investigate the impact of metal element content on tomato quality, Zhang et al. proposed a positive matrix factorization model. They measured metal content in tomato samples, used the model to analyze pollution sources and distribution, and combined it with the ecological risk index to evaluate risk levels [11]. To detect rare earth elements in plants, Falandysz designed a novel inductively coupled plasma emission spectrometer. Plant samples were collected, weighed, digested with nitric acid using microwave digestion, diluted and filtered, and the rare earth characteristic spectral lines were measured to calculate rare earth content [12]. To evaluate metal pollution in soil, Huang et al. proposed a method combining K-means clustering and SVM. They measured metal content in soil samples, used K-means clustering to divide pollution regions, and modeled pollution degree with SVM [13]. For analyzing metal values in rice, an inductively coupled plasma mass spectrometry technique analysis was conducted by Navaretnam et al. The rice sampless were digested, and values of metal element were calculated by using a technique to analyze the degree of contamination and safety [14]. For analyzing fluidity in aluminum alloys in iron, a fusion model based on multiple algorithms was put forward by Durmuş et al., who gathered iron-aluminum alloy samples, calculated parameters, modeled variables with multiple algorithms, simulated aluminum fluidity, and analyzed fluidity [15]. Based on the above content, it can be concluded that existing research methods still face three core scientific problems in the assessment of heavy metal content in farmland soils: firstly, traditional univariate analysis methods and basic statistical models are difficult to capture the nonlinear dynamic interaction between heavy metal elements and soil environmental factors; Secondly, existing intelligent models are susceptible to interference features when processing high-dimensional temporal data, and the randomness of parameter initialization makes the model prone to falling into local optima; Thirdly, the collaborative mechanism between the modules of the composite model is not yet clear, and there is a lack of a systematic framework for evaluating multi-source data fusion. Therefore, this study proposed applying the GElman algorithm to assess farmland heavy metal content. By using GWO to optimize Elman's key parameters, the model enhanced the linkage between soil environmental factors and heavy metal content. The core innovative contributions of the research are as follows: Firstly, the combination of GWO and genetic algorithm improved particle swarm optimization algorithm forms a two-layer hybrid optimization strategy for global optimization and local fine-tuning of Elman network parameters, effectively solving the problem of premature convergence of a single optimization algorithm. Secondly, introducing gate controlled recurrent units to improve the random forest model and integrating convolutional block attention mechanism enhances the joint modeling ability of the model for temporal features and static nonlinear interactions while retaining the advantages of random forest ensemble learning, and suppresses interference features through channel and spatial attention. Thirdly, a complete evaluation process from data preprocessing, feature extraction, attention filtering to parameter optimization has been constructed, forming an end-to-end evaluation framework with good reproducibility.

2. Methods

2.1. Farmland heavy metal content assessment model based on GElman algorithm

2.1.1. Optimization design of GElman algorithm based on improved PSO

Farmland heavy metal content assessment usually relies on the nonlinear mapping relationship between environmental factors and metal elements. The GElman algorithm, which combines GWO and Elman, balances local features and metal element recognition ability through a collaborative mechanism of dynamic neurons and key feature weight optimization. Therefore, this study applies the GElman algorithm to farmland heavy metal content assessment. Its operation process is shown in Figure 1.

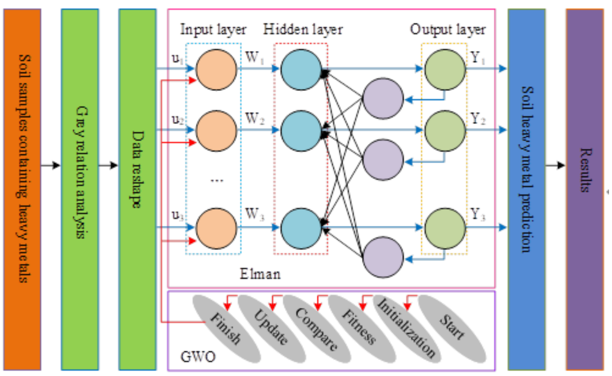

Fig. 1. Evaluation process of heavy metal content in farmland based on GElman algorithm

As shown in Fig. 1, the GElman algorithm first preprocesses soil samples containing heavy metals. Then it sets the Elman structure and GWO parameters, encodes network weights, updates positions using GWO, iteratively searches for optimal parameters, and inputs them into Elman for training. If heavy metal assessment accuracy meets the standard, the output is generated; otherwise, optimization is repeated. The specific preprocessing steps are as follows: for missing values in the original data, multiple imputation is used to fill them, that is, using information from other related variables to estimate missing values through regression models, in order to preserve sample information to the greatest extent possible. For outliers, the quartile range method is used for identification. Values below 1.5 times the quartile range of the first quartile or above 1.5 times the quartile range of the third and fourth quartiles are considered outliers and corrected based on the mean of adjacent normal values. To eliminate the influence of dimensional differences between different heavy metal elements and soil physicochemical parameters on model training, minimum maximum normalization is applied to the input features, and each feature value is linearly transformed into the [0,1] interval. In terms of sample balance, due to the natural differences in the distribution of heavy metal elements in soil, this study did not artificially balance the samples, but retained the original distribution characteristics to reflect the proportion relationship of heavy metal content in the real soil environment. GWO position update calculation is shown in Eq. (1).

$$X(t+1) = X_p(t) - A \cdot D \tag{1}$$

In Eq. (1), X represents candidate solutions, X_p represents the optimal solution, A represents the update direction, t is the number of position updates, and D is the update distance. A fitness function evaluates the data to guide the GWO search direction, calculated as shown in Eq. (2).

$$\text{fitness} = RMSE = \sqrt{\frac{\sum_{i=1}^{n}(y_i - \overline{y_i})^2}{N}} \tag{2}$$

In Eq. (2), N represents sample size, y_i represents actual values, and $\overline{y_i}$ represents predicted values. The hidden layer state of Elman network not only depends on the current input vector, but also introduces the output state of the hidden layer at the previous moment through the receiving layer. This recursive structure enables the network to have short-term memory ability, which can continuously transmit historical information to subsequent time steps, thus maintaining a continuous representation of the dependency relationship before and after the sequence during the dynamic change process of soil heavy metal content modeling. This feature is precisely the core advantage of

Elman networks over feedforward neural networks in processing temporal data. The specific calculation formula is shown in Eq. (3).

$$s(t) = f\left(w_1 \cdot x(t) + w_2 \cdot c(t-1) + b_1\right) \tag{3}$$

In Eq. (3), $x(t)$ is the input vector of the output layer, $c(t-1)$ represents the state vector of the context layer, w_1 and w_2 represent weight matrices of the hidden and context layers, b_1 represents the hidden layer bias vector, and $f(\cdot)$ represents the activation function. During data processing, the GElman algorithm utilizes the global search capability of the grey wolf optimizer to assist the Elman neural network in locating the global optimal parameters. The grey wolf optimizer uses a group collaboration mechanism and position update strategy to reduce the randomness in the Elman network parameter initialization process and enhance the algorithm's robustness to different initial parameters. However, GElman relies heavily on GWO's search ability, which reduces its fitting capability for complex data in later iterations and slows convergence in high-dimensional parameter space. The Particle Swarm Optimization (PSO) algorithm improved by Genetic Algorithm (GA) can locate a better search space and perform fine search within this space using its fast convergence and local search ability. The optimized parameters are then applied to the target network. Therefore, this study introduces improved PSO into the GElman algorithm. The operation process of improved PSO is shown in Fig. 2.

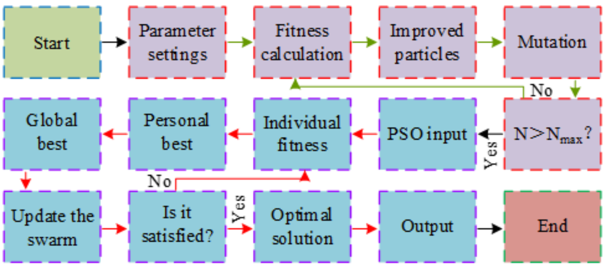

Fig. 2. Location of the KVMRT project

As shown in Fig. 2, the improved PSO algorithm uses GA's genetic mechanism to maintain diversity in the PSO population and optimizes locally through PSO's search ability, improving convergence speed and accuracy in the target area. GA selection for data is calculated as shown in Eq. (4).

$$P_i' = \frac{fit_i - f_{\min}}{\sum_{i=1}^{N}\left(fit_i - f_{\min}\right)} \tag{4}$$

In Eq. (4), $f_{\min}$ represents the worst fitness value, $fitt_i$ represents the current fitness value, and N represents the total number of individuals in the population. PSO updates the velocity of optimal particles as shown in Eq. (5).

$$v_{ij}(t+1) = v_{ij}(t) + c_1 r_1(t)\left[p_{ij}(t) - x_{ij}(t)\right] + c_2 r_2(t)\left[p_{ij}(t) - x_{ij}(t)\right] \tag{5}$$

In Eq. (5), c_1 and c_2 represent learning factors, r_1 and r_2 represent uniform random numbers, p_{ij} represents the optimal position found, and x_{ij} represents the position. The inertia weight of improved PSO is expressed as shown in Eq. (6).

$$w^k = S(k)w_{\min} + \left[\frac{k\left(w_{\max} - w_{\min}\right)}{k_{\max}}\right] \tag{6}$$

In Eq. (6), k is the current iteration, $w_{\max}$ and $w_{\min}$ represent upper and lower limits of inertia weight, and $S(k)$ represents chaotic mapping. The improved PSO algorithm iteratively optimizes particles to generate new PSO particles, reconnecting nonlinear influences among particles, and uses GA to search low-dimensional space. GElman improves assessment accuracy by optimizing model parameters and learning the mapping relationships among factors. Therefore, this study combines GElman with improved PSO to form the RGElman algorithm. Its operation process is shown in Fig. 3.

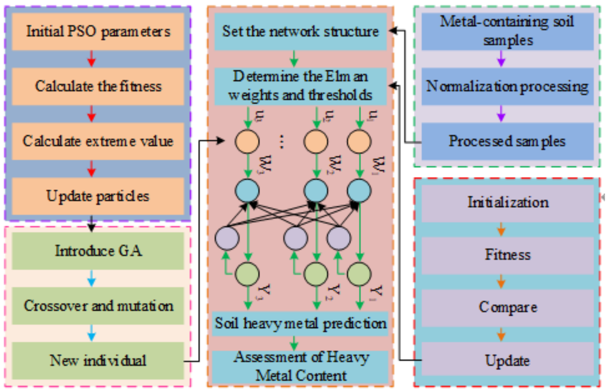

Fig. 3. PGElman algorithm operation flow chart

As shown in Fig. 3, the PGElman algorithm first determines the Elman structure, then uses improved PSO to optimize the particle swarm, retaining the best individuals to select optimal weights and thresholds for Elman. GWO further optimizes the network structure, and finally outputs the soil metal content assessment. Particle fitness is calculated as shown in Eq. (7).

$$f = \sum_{i=1}^{1} abs\left(t_i - z_i\right) \tag{7}$$

In Eq. (7), f represents individual fitness value, t_i represents network prediction output, and z_i represents expected output. During weight adjustment in Elman, GA mutates the genetic code of the j-th segment in the i-th sample, as shown in Eq. (8).

$$\begin{cases} p_{ij} = p_{ij} + \left(p_{ij} - p_{\max}\right) \times f(g), & r \geq 0.5, \\ p_{ij} = p_{ij} + \left(p_{\min} - p_{ij}\right) \times f(g), & r \leq 0.5. \end{cases} \tag{8}$$

In Eq. (8), $p_{\max}$ represents the upper bound of the gene, $p_{\min}$ represents the lower bound, g represents the current evolution generation, and r is any number between 0 and 1. Improved PSO places particles in a specific -dimensional space, as shown in Eq. (9).

$$D = l \times m + m \times n + m + n \tag{9}$$

In Eq. (9), l represents the number of input nodes in Elman, m represents the number of hidden layer nodes. During heavy metal content assessment, the GA-PSO algorithm, with global optimization and genetic mechanism, optimizes potential correlation features of metal distribution, expands understanding of spatial distribution, compensates for GElman's limitations in capturing correlation features in complex soil environments, and improves the accuracy and comprehensiveness of farmland heavy metal content assessment.

2.1.2. *Construction of heavy metal content assessment model based on PGElman algorithm*

After the completion of the RGEIman algorithm design, its core component Elman neural network mainly achieves dynamic memory in the time dimension through the receptive layer, focusing on capturing temporal dependencies in sequential data. In the practical scenario of assessing heavy metal content in farmland soil, the interaction between heavy metal elements and soil physicochemical properties often exhibits complex non temporal and nonlinear characteristics. Simply increasing the depth or adjusting the internal structure of Elman networks can improve their nonlinear fitting ability to a certain extent. However, due to the time backpropagation mechanism of their recursive networks, increasing the depth of the network carries the risk of gradient vanishing or exploding, and it is difficult to effectively model the non temporal and static complex interaction relationships between input features. Therefore, this study introduces a Random Forest (RF) model improved by Gated Recurrent Unit (GRU). Among them, RF can capture high-order nonlinear interactions between features without relying on temporal assumptions through the ensemble learning mechanism of multiple decision trees; The GRU module is used to extract high-dimensional temporal features from input data to supplement RF's insufficient modeling of dynamic change information. The operation process of improved RF is shown in Fig. 4.

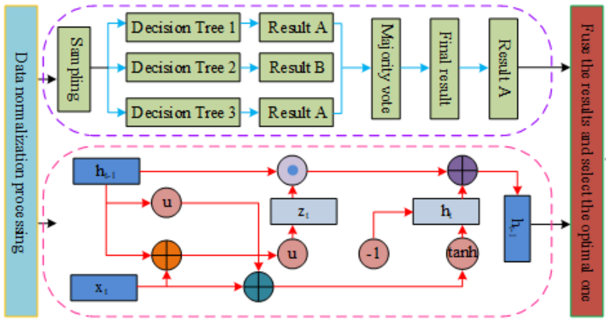

Fig. 4. Improved RF operation flow chart

As shown in Fig. 4, during data processing, the data enter the GRU module and RF module separately. The GRU module extracts high-dimensional data, performs interactions, and concatenates them with other features. The RF module calculates optimal results using multiple decision tree strategies and differentiated parameters. The best results from both modules are fused to select the optimal solution. When dividing data attributes, improved RF uses the Gini index as the criterion, calculated as shown in Eq. (10).

$$\mathrm{Gini}(D) = 1 - \sum_{k=1}^{K} \left(\frac{|C_k|^2}{|D|}\right) \tag{10}$$

In Eq. (10), D represents the sample set, k represents the number of categories, and C_k represents the subset of samples in D that belong to the k-th category. The GRU vulnerability detection layer uses feature input from the fusion layer into the Soft max function to generate detection results. The Soft max function is shown in Eq. (11).

$$\mathrm{Soft\ max}\,(Z_i) = \frac{e^{Z_i}}{\sum_{c=1}^{C} e^{Z_C}} \tag{11}$$

In Eq. (11), Z_i represents the output value, C is the number of categories, and e represents the feature value from the fusion layer. RF generates decision trees as shown in Eq. (12).

$$\mathrm{Tree}_{\ k} = \ \mathrm{DecisionTree}\ \left(D_i, F_j\right) \tag{12}$$

In Eq. (12), D_i represents the sample subset randomly selected from the original dataset, and F_j represents the feature subset randomly selected from the original feature set. After introducing RF and GRU, the overall depth and feature dimension of the network significantly increased in the above model, resulting in the synchronous extraction of some interference features unrelated to heavy metal content assessment, which reduced the model's attention to key environmental factors. Although deepening the Elman network also faces similar interference feature problems, its recursive structure lacks an explicit feature reweighting mechanism. Therefore, the study further introduces the Convolutional Block Attention Module (CBAM), which adaptively filters and enhances the intermediate layer features of the composite model through dual pooling operations of channel attention and spatial attention, thereby improving the expression efficiency of key features and suppressing invalid interference information without changing the main structure of the model. The process of reducing interference features using CBAM is shown in Fig. 5.

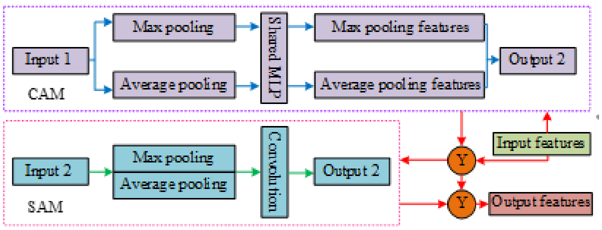

Fig. 5. Schematic diagram of the CBAM process for reducing interference features

As shown in Fig. 5, features with interference enter the channel attention module. All features undergo max pooling and average pooling. The channel is first compressed to filter interference features. The filtered features enter the spatial attention module, undergo a second pooling operation, and the processed features are concatenated and output. Channel attention is calculated as shown in Eq. (13).

$$M_c(F) = \sigma \left(W_1 \left(W_0 \left(F^c_{\text{avg}} \right) \right) + W_1 \left(W_0 \left(F^c_{\max} \right) \right) \right) \quad (13)$$

In Eq. (13), σ represents the channel activation function, F^c_{avg} and $F^c_{\max}$ represent average-pooled and max-pooled features, and W_0 and W_1 represent shared weights. Spatial attention is shown in Eq. (14).

$$M_s(F) = \eta \left(f^{7\times 7} \left(\left[F^c_{\text{avg}} ; F^c_{\max} \right] \right) \right) \quad (14)$$

In Eq. (14), η represents the spatial activation function, and $f^{7\times 7}$ represents the convolution kernel size. The receptive field in the compressed channel can be expanded as calculated in Eq. (15).

$$G_i = (G_{i+1} - 1) \times \text{ stride }_i + \text{ Ksize }_i \quad (15)$$

In Eq. (15), G_{i+1} represents the receptive field at layer $i+1$, stride $_i$ represents the convolution stride, and Ksize_i represents the stride of the convolution kernel in this layer. CBAM uses dual pooling operations to effectively filter invalid features in improved RF, enhancing model stability, training accuracy, and efficiency. Combined with PGElman, it achieves precise assessment of farmland heavy metal content. Therefore, this study integrates the algorithms to propose the CRF-PGElman model. Its operation process is shown in Fig. 6.

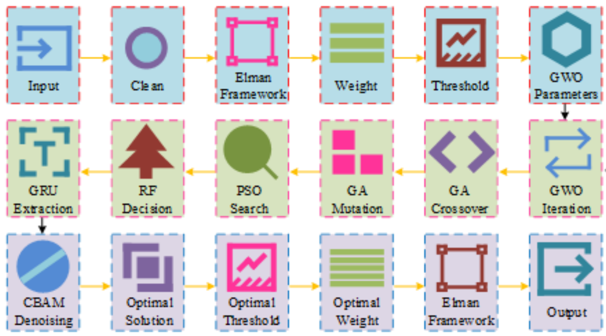

Fig. 6. Schematic diagram of the evaluation process of the CRF-PGEIman model

As shown in Fig. 6, GA-PSO performs global optimization of key parameters in heavy metal content assessment through the collaborative mechanism of particle swarm optimization and genetic evolution, capturing factors that affect assessment accuracy. GRU-RF captures temporal features and uses classification-regression characteristics to dynamically associate farmland environmental data, improving prediction stability for heavy metal content trends. CBAM strengthens the feature weight allocation for key environmental factors through channel and spatial attention, reducing interference from invalid data. GWO-Elman combines global search capability and Elman's dynamic memory, optimizing network parameters iteratively and improving the fitting of nonlinear mapping relationships for farmland heavy metal content, ultimately outputting the assessment results. In summary, the CRF-PGElman model captures influencing factors and dynamic variation patterns of heavy metal content, achieving accurate assessment and providing strong technical support for farmland soil pollution control.

3. Results and discussion

3.1. Experimental details

To verify the superior performance of the PGElman algorithm in assessing farmland heavy metal content, the study compared it with Artificial Bee Colony-Extreme Learning Machine (ABC-ELM), Gravitational Search Algorithm-Back Propagation Neural Network (GSA-BP), and Ant Colony Optimization-Radial Basis Function Neural Network (ACO-RBF).

All experiments were conducted on high-performance computing servers configured with NVIDIA Tesla A800 (40 GB of video memory) and 256 GB of memory. The software environment adopts Windows 11 operating system, PyTorch deep learning framework, and Python 3.12. x , and the Adam optimizer is uniformly used during the model training process.

To ensure the reliability of model evaluation, the study adopted the spatial distribution characteristics dataset of heavy metals in farmland soil in China as the training set, and another independently collected dataset of heavy metal content distribution in soil as the validation set. Both datasets cover a variety of soil types and heavy metal distribution information under different environmental conditions, providing a data basis for the robustness test of the model in different soil environments. The training set was collected by relevant research institutions from 2018 to 2020 in major agricultural areas across the country (including the North China Plain, the Middle and Lower Reaches of the Yangtze River Plain, and the Northeast Black Soil Region), and contains a total of 1,247 soil samples. Each sample records the content of seven heavy metal elements, including copper (Cu), nickel (Ni), lead (Pb), zinc (Zn), iron (Fe), chromium (Cr), and mercury (Hg), as well as soil physical and chemical property parameters such as pH value, organic matter content, and cation exchange capacity. The content range of heavy metals is as follows: Cu is $5.2 - 156.3$mg/kg, Ni is $4.8 - 112.6$mg/kg, Pb is $10.5 - 298.4$mg/kg, Zn is $22.3 - 389.7$mg/kg, Fe is $1.2 - 8.9$ g/kg, Cr is $12.4 - 198.7$mg/kg, and Hg is $0.02 - 1.56$mg/kg. The validation set uses an independently collected dataset of heavy metal content distribution in soil, containing 312 samples, with the sampling time consistent with the training set and the sampling points distributed in line with the main agricultural areas in China to ensure the independence of the validation results. In addition, the experiment uses the European agricultural soil heavy metal concentration dataset as the training set and the heavy metal content dataset of farmland and crops in the Moquegua mining area of Peru as the experimental set. Both datasets cover a variety of agricultural soil and crop samples and can be used to evaluate metal content in different farmland scenarios. The training set is from the EU Soil and Environment Monitoring Project, collected from 2017 to 2019 in major agricultural areas in Europe (including France, Germany, Poland, Spain, etc.), and contains a total of 892 soil samples, covering the same heavy metal elements and physical and chemical parameters as the aforementioned Chinese dataset. The experimental set uses the heavy metal content dataset of farmland and crops in the Moquegua mining area of Peru, which was collected by local environmental monitoring agencies from 2019 to 2021, and contains a total of 456 soil samples and corresponding crop samples (mainly corn and potatoes). This area has a high content of heavy metals in the soil due to long-term mining activities, with the following content range of heavy metals: Cu is $18.6 - 342.5$mg/kg, Pb is $25.3 - 568.7$mg/kg, Zn is $35.8 - 612.4$mg/kg, Fe is $2.5 - 15.6$ g/kg, Cr is $8.9 - 245.3$mg/kg, and Hg is $0.05 - 3.24$mg/kg. The above datasets cover different climate types such as temperate monsoon climate, Mediterranean climate, and tropical desert climate, as well as major soil types such as black soil, brown soil, red soil, and alluvial soil. Through the combined use of these datasets, the model's evaluation performance in different soil types, pollution backgrounds, and geographical regions can be effectively simulated, demonstrating strong representativeness. The content range of heavy metals in all samples covers the complete gradient from background values to pollution levels, providing a data basis for the robustness verification of the model under diverse conditions.

3.2. Performance of farmland heavy metal content assessment model based on PGEIman

3.2.1. *Effective validation of PGElman algorithm*

The study predicted the contents of copper (Cu), nickel (Ni), lead (Pb), and zinc (Zn) in a soil sample and compared them with actual values. The results are shown in Fig. 7.

As shown in Fig. 7, for Cu density prediction, PGElman closely matched the actual density. In a 0.9 m^2 soil sample, PGElman predicted a Cu density of 1.4, identical to the real value. The predicted Ni values by PGElman were also close to the actual Ni density, while GSA-BP generally overestimated and ACO-RBF underestimated. For Pb and Zn density prediction, PGElman's results were close to actual values. Overall, PGElman demonstrated strong convergence in testing. Its excellent performance resulted from combining GA's global search ability with PSO's local optimization, which allowed PGElman to avoid local optima and achieve high prediction accuracy. Next, the study tested error rate and accuracy. The results are shown in Fig. 8.

In Fig. 8(a), with the increased iterations, the accu-

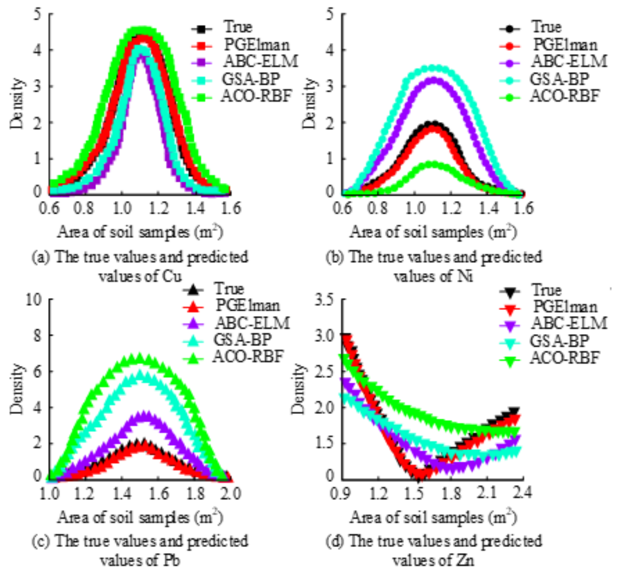

Fig. 7. Comparison of actual and predicted values of soil heavy metal content

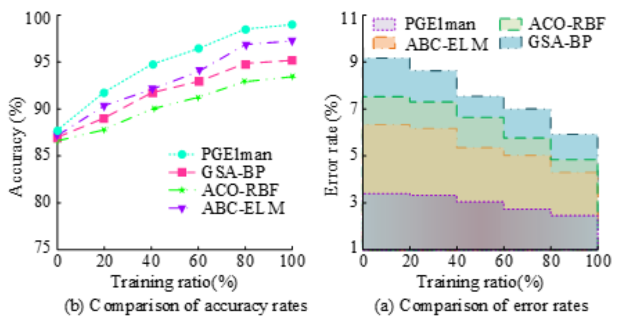

Fig. 8. Comparison of accuracy and error rate test results

racies of PGElman, GSA-BP, ACO-RBF, and ABC-ELM reached 99.5%, 96.22%, 93.1%, and 92.9%, respectively. From Fig. 8(b), it can be noted that PGElman had less error rate, which was only 2.9%, whereas GSA-BP had the highest error rate of 6.1%, which reached 9.1% in initial iterations. ACO-RBF and ABC-ELM performed relatively better, and their final error rate stood at 5.1% and 4.7%, respectively. PGElman performed better than other compared models, and it showed better robustness and adaptability in this task. The robustness shown by PGElman caused by its model, CBAM, allowed adequate feature representation with suppression of unnecessary interference. The precision and recall values are presented in Fig. 9.

In Fig. 9, the closer the top-right point to coordinates $(1, 1)$, the better the performance. A higher Area Under Curve (AUC) indicated better performance. As shown in Fig. 9(a) and (b), PGElman achieved AUC values of 0.94

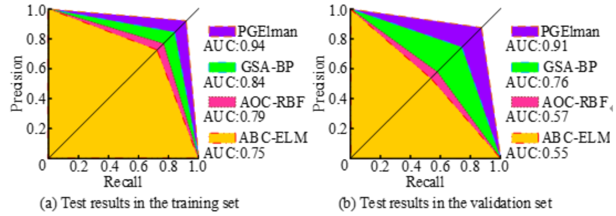

Fig. 9. Comparison of precision and recall test results

and 0.91 across different datasets, outperforming comparative models. In the training set, the top-right coordinate was $(0.98, 0.98)$, indicating both precision and recall were 0.98, significantly higher than the other models. ABC-ELM performed worst, with AUCs of 0.75 and 0.55 . These results verified PGElman's strong fitting ability, attributable to GWO's global optimization avoiding local optima and Elman's dynamic memory enabling better sequence modeling.

3.2.2. *Evaluation analysis of PGElman farmland heavy metal content assessment model*

After validating PGElman's performance, the study further assessed the farmland heavy metal content evaluation model built on PGElman. The study tested recognition accuracy of iron (Fe), chromium (Cr), and mercury (Hg), labeled as A, B, and C , respectively. The results are shown in Fig. 10.

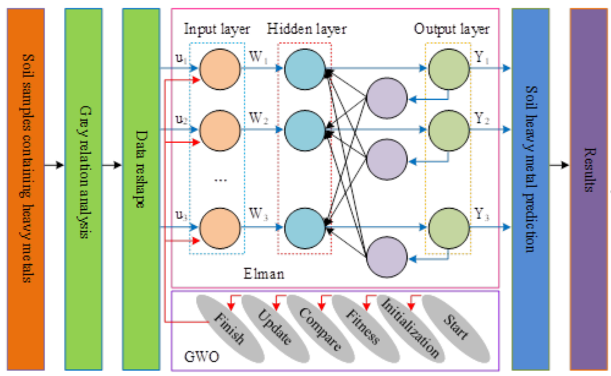

Fig. 10. Recognition accuracy confusion matrix

As shown in Fig. 10(a), PGElman achieved recognition accuracies of 0.99, 0.98 , and 0.99 for Fe, Cr, and Hg , respectively. For Cr , misclassification as Fe or Hg occurred with a probability of 0.01 . Fig. 10(b) and (c) showed that ABC-ELM and GSA-BP had lower recognition accuracy, with GSA-BP achieving only 0.79 for Hg . Fig. 10(d) showed that ACO-RBF reached a maximum recognition accuracy of 0.96 for some metals but still fell below PGElman. Overall, PGElman demonstrated strong generalization and fitting ability in recognition tests, owing to the integration of GRU's temporal feature capture and RF's ensemble decision-making, which enabled precise identification of dynamic correlations among metal elements. The study then predicted heavy metal contents in a soil sample and compared predicted values with actual contents, as shown in Fig. 11.

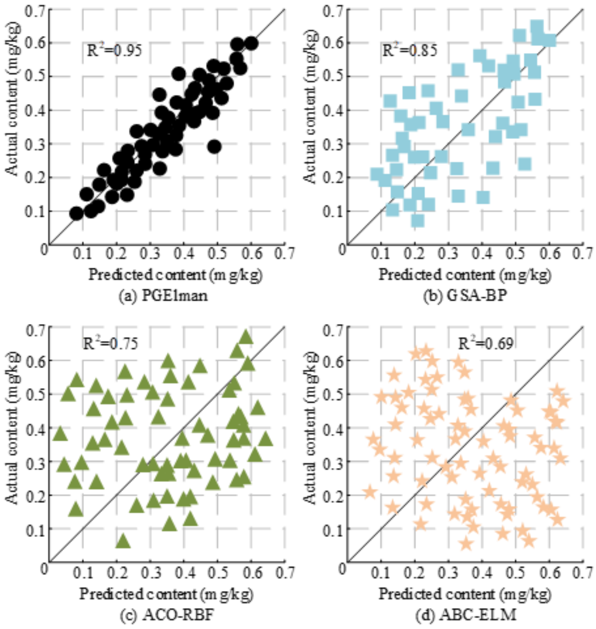

Fig. 11. Comparison of predicted results and actual heavy metal content

In Fig. 11, the diagonal represents actual values, and the distribution represents predicted values. A Coefficient of Determination (R^2) closer to 1 indicates stronger model performance. From Fig. 11(a), (b), (c), and (d), the R^2 value for PGElman, GSA-BP, ACO-RBF, and ABC-ELM was 0.95, 0.85, 0.75, and 0.69, respectively. The PGElman predicted results were closely aligned with the diagonal. However, ACO-RBF and ABC-ELM results are scattered, representing larger deviations from actual values. These findings confirm that PGElman outperformed the comparative models due to its potential for parameter optimization and dynamic sequence learning that allow for accurately tuning the network parameters and capturing nonlinear dependencies in data. Finally, the study has compared precision, recall, and F1 scores. Results are presented in Fig. 12.

As can be seen from Fig. 12(a), the precision, recall, and F1 score of PGElman on the validation set are 99.24%, 99.01%, and 99.12%, respectively, which further confirmed its stability between different datasets. Fig. 12(b), (c), and (d) indicate that GSA-BP and ABC-ELM has bad performance, while the ACO-RBF has a good result with the precision of 98.14%, recall of 97.67%, and F1 score of

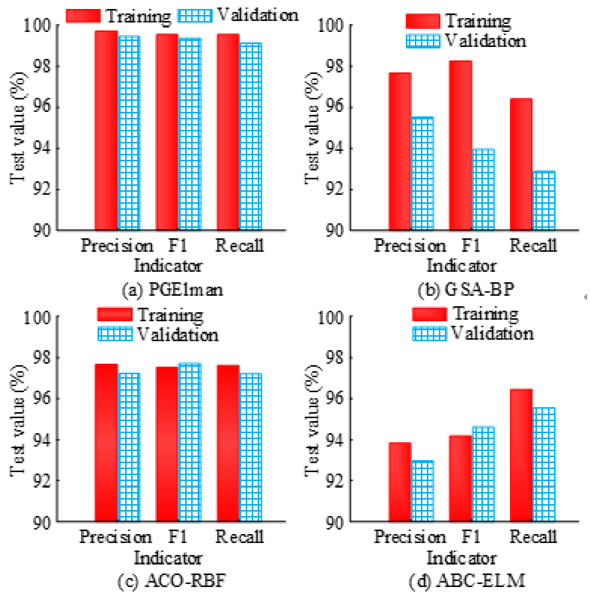

Fig. 12. Results of different comprehensive indicators in two datasets

98.52%. To clarify the actual contributions of each component module in the CRF PGElman model to overall performance, ablation experiments were designed and studied. Under the premise of maintaining the same experimental environment and dataset, gradually remove or replace specific modules to evaluate the impact of each module on evaluation accuracy, error rate, and R^2. The results are shown in Table 1.

85.3%, with an error rate of 12.1%, indicating that the unoptimized Elman model has significant shortcomings in the task of assessing heavy metal content in farmland. After introducing GWO optimization (Model B), the accuracy increased to 92.7%, the error rate decreased to 6.8%, and the R^2 increased to 0.81 , verifying the effectiveness of GWO in global parameter optimization. After further introducing GA-PSO optimization (Model C, i.e. PGElman), the accuracy was significantly improved to 99.5%, the error rate was reduced to 2.9%, and the R^2 reached 0.95 , indicating that the GA-PSO hybrid optimization strategy significantly enhanced the model's parameter optimization ability and convergence accuracy. On the basis of PGElman, GRU is introduced to improve the random forest (Model D), with a slight increase in accuracy to 99.6% and an increase in R^2 to 0.96 , indicating that the GRU-RF module's modeling ability for nonlinear interaction features has to some extent supplemented the shortcomings of PGElman. After introducing CBAM, the complete model E achieved an accuracy of 99.7% and an R^2 of 0.97 . Although the improvement

Table 1. Results of ablation experiment

Mode	Module Composition	Accuracy (%)	Error rate (%)	R^2
A	Elman	85.3	12.1	0.62
B	Elman + GWO	92.7	6.8	0.81
C	Elman + GWO + GA-PSO	99.5	2.9	0.95
D	PGEIman + GRU-RF	99.6	2.7	0.96
E	PGEIman + GRU-RF + CBAM (CRF-PGEIman)	99.7	2.5	0.97

compared to model D was limited, the error rate was further reduced by 0.2%, indicating that CBAM played a fine tuning role by suppressing interference features. In summary, the ablation experiment results indicate that each module contributes positively to the overall performance of the CRF PGElman model, with the optimized combination of GA-PSO and GWO making the most significant contribution. The GRU-RF and CBAM modules can still provide marginal gains even after the basic model achieves high performance. This result validates the rationality of the model design and the necessity of the existence of each module.

To verify the final performance of the CRF PGElman model, independent testing was conducted on the same experimental environment and dataset. Training and validation were conducted using the spatial distribution characteristics dataset of heavy metals in Chinese farmland soil and independent soil heavy metal content distribution data, and compared with PGElman, ABC-ELM, GSA-BP, and ACO-RBF models. The evaluation indicators include accuracy, error rate, Mean Absolute Error (MAE), Root Mmean Square Error (RMSE), and R^2. The results are shown in Table 2.

According to Table 2, the CRF PGElman model outperforms PGElman and other comparative models in all indicators. Compared with PGElman, the accuracy of CRF PGElman increased from 99.5% to 99.7%, the error rate decreased from 2.9% to 2.5%, the R^2 increased from 0.95 to 0.97 , and the MAE and RMSE decreased by 25.0% and 19.5%, respectively. This is mainly due to the introduction of GRU-RF and CBAM attention modules in the CRF PGElman model. GRU-RF enhances the joint modeling ability of the model for high-dimensional temporal features and static nonlinear interactions, while CBAM effectively suppresses interference features in deep networks through channel and spatial attention mechanisms, thereby further improving evaluation accuracy and stability. The above results indicate that the CRF PGElman model, as the final proposed complete model in this paper, has the best comprehensive performance in the task of assessing heavy metal content in farmland soil. In summary, PGElman has the best performance among all comparative models, confirming its comprehensive performance and stability. The advantages originated from the mechanism of maintaining population diversity of GA and information collaboration efficiency of PSO, providing a guarantee for PGElman to avoid getting trapped into premature convergence and accelerate the optimization process.

4. Conclusion

On the basis of the present deficiencies in the dynamic assessment of farmland heavy metal content, an algorithm for evaluating metal content based on PGElman was put forward in the research, as well as a model to match the algorithm. The model involved data preprocessing of the original values of farmland heavy metal content. GRU extracted the patterns of metal content dynamics in the data, RF improved feature screening and conducted nonlinear transformation, GA-PSO carried out dynamic optimization of feature sequences, and GWO conducted collaborative optimization of Elman model parameters. During this process, CBAM filtered interfering data using channel attention, and the final output provided the assessment of farmland heavy metal content. Tests have shown that the RF PGElman model has an evaluation accuracy of 99.7%, an error rate of 2.5%, a MAE of 0.21mg/kg, an RMSE of 0.33mg/kg, and an R^2 of 0.97 , significantly better than traditional combination models such as ABC-ELM $\left(R^2 = 0.69\right)$, GSA-BP $\left(R^2 = 0.85\right)$, and ACO-RBF $\left(R^2 = 0.75\right)$. In cross regional validation, the model achieved recognition accuracies of 0.99, 0.98, and 0.99 for iron, chromium, and mercury, respectively, verifying its generalization ability in geographical backgrounds different from the training set. The ablation experiment further confirmed that the optimized combination of GA-PSO and GWO made the most significant contribution to the model performance. After introducing this optimization strategy, the accuracy increased from 85.3% to 99.5%; The GRU-RF and CBAM modules can still provide marginal gain after achieving high performance in the base model, further improving accuracy to 99.6% and 99.7%, respectively. The above results fully demonstrate the effectiveness of the proposed model in dynamic sequence modeling, nonlinear interaction capture, and multi-source data fusion evaluation. However, there are still certain

Table 2. Comparison of final performance of different methods

Model	Accuracy (%)	Error rate (%)	MAE (mg/kg)	RMSE (mg/kg)	R^2
ABC-ELM	92.9	4.7	0.87	1.23	0.69
GSA-BP	96.2	6.1	0.76	1.09	0.85
ACO-RBF	93.1	5.1	0.81	1.14	0.75
PGEIman	99.5	2.9	0.28	0.41	0.95
CRF-PGEIman	99.7	2.5	0.21	0.33	0.97

limitations in the research. When deploying the model for large-scale soil pollution monitoring, it may face higher requirements for computational resources and data collection capabilities, such as high-density sampling and multi-element synchronous analysis required for large-scale monitoring; In addition, in areas lacking representative training samples, the accuracy of its evaluation may be limited. At the same time, the model has a strong dependence on the quality of training data, including the representativeness of samples, the accuracy of heavy metal content determination, and the completeness of soil physicochemical parameter collection. Low quality or biased data input may lead to significant deviation of evaluation results from the true values. The model is composed of multiple modules, with a large number of parameters. The inference process involves multiple iterations of optimization and feature transformation, resulting in high computational complexity. Future work can improve the robustness and evaluation accuracy of the model in complex scenarios by collecting more cross regional and multi environmental soil heavy metal data, retraining and parameter optimization. In addition, exploring data augmentation techniques and transfer learning methods can reduce the model's dependence on high-quality annotated data and enhance its applicability in data scarce areas. And carry out research on model lightweighting, such as reducing computational complexity and improving inference efficiency through knowledge distillation, network pruning, or module simplification.

References

[1] M. Singh, (2024) *"Exploring the possibilities to implement metaverse in higher education institutions of India"* **Education and Information Technologies** ***29***(15): 20715–20728. DOI: 10.1007/s10639-024-12691-2.

[2] S. P. Suryodiningrat, H. Prabowo, A. Ramadhan, and H. B. Santoso, (2024) *"The Essential Components of Metaverse-based Mixed Reality for Machinery Vocational Schools"* **Journal of Applied Engineering Technology and Science** *5*(2): 1069–1085. DOI: 10.37385/jaets.v5i2.4117.

[3] A. M. Farouk, H. Naganathan, R. A. Rahman, and J. Kim, (2024) *"Exploring the Economic Viability of Virtual Reality in Architectural, Engineering, and Construction Education"* **Buildings** ***14***(9): 2655. DOI: 10.3390/buildings14092655.

[4] G. Lampropoulos, (2025) *"Combining Artificial Intelligence with Augmented Reality and Virtual Reality in Education: Current Trends and Future Perspectives"* **Multimodal Technologies and Interaction** ***9***(2): 11. DOI: 10.3390/mti9020011.

[5] H. Lee and Y. Hwang, (2022) *"Technology-Enhanced Education through VR-Making and Metaverse-Linking to Foster Teacher Readiness and Sustainable Learning"* **Sustainability** ***14***(8): 4786. DOI: 10.3390/su14084786.

[6] C. O. Nwamekwe and E. C. Nwabunwanne, (2025) *"Immersive Digital Twin Integration in the Metaverse for Supply Chain Resilience and Disruption Management"* **Journal of Engineering Research and Applied Science** ***14***(1): 95–105. DOI: 10.0000/placeholder-doi.

[7] P. Onu, A. Pradhan, and C. Mbohwa, (2024) *"Potential to use metaverse for future teaching and learning"* **Education and Information Technologies** ***29***(7): 8893–8924. DOI: 10.1007/s10639-023-12167-9.

[8] F. Shi et al., (2024) *"A new technology perspective of the Metaverse: Its essence, framework and challenges"* **Digital Communications and Networks** ***10***(6): 1653–1665. DOI: 10.1016/j.dcan.2023.02.017.

[9] C.-H. Wang, (2025) *"Education in the metaverse: Developing virtual reality teaching materials for K–12 natural science"* **Education and Information Technologies** ***30***(7): 8637–8658. DOI: 10.1007/s10639-024-13156-2.

[10] M. Muthmainnah, L. Cardoso, A. G. Marzuki, and A. Al Yakin, (2025) *"A new innovative metaverse ecosystem: VR-based human interaction enhances EFL learners' transferable skills"* **Discover Sustainability** ***6***(1): 156. DOI: 10.1007/s43621-025-00913-7.

[11] M. Singh, D. Sun, and Z. Zheng, (2024) *"Enhancing university students' learning performance in a metaverse-enabled immersive learning environment for STEM edu-*

cation: A community of inquiry approach" **Future Education Research** *2*(3): 288–309. DOI: 10.1002/fer3.56.

[12] J. Lee and Y. Kim, (2023) *"Sustainable Educational Metaverse Content and System Based on Deep Learning for Enhancing Learner Immersion"* **Sustainability** ***15***(16): 12663. DOI: 10.3390/su151612663.

[13] A. Waqar et al., (2023) *"Analyzing the Success of Adopting Metaverse in Construction Industry: Structural Equation Modelling"* **Journal of Engineering** ***2023***: 1–21. DOI: 10.1155/2023/8824795.

[14] N. Bartels and K. Hahne, (2023) *"Teaching Building Information Modeling in the Metaverse—An Approach Based on Quantitative and Qualitative Evaluation of the Students Perspective"* **Buildings** ***13***(9): 2198. DOI: 10.3390/buildings13092198.

[15] Z. Liu, S. Gong, Z. Tan, and P. Demian, (2023) *"Immersive Technologies-Driven Building Information Modeling (BIM) in the Context of Metaverse"* **Buildings** ***13***(6): 1559. DOI: 10.3390/buildings13061559.